On-Wafer Characterization, Modelling, and Optimization of InP-based HEMTs, pin-Photodiodes and Monolithic Receiver-OEICs for Fiber-Optic Communication

D. Kaiser, H. Grosskopf, I. Gyuro, U. Koerner, W. Kuebart, J.-H. Reemtsma,
and H. Eisele

Alcatel-SEL, Research Center, Optoelectronics Division
D-7000 Stuttgart 40, Lorenzstr.10, Germany

We will demonstrate results achieved with receiver-OEICs consisting of InGaAs pin-photodiodes and InAlAs/InGaAs HEMTs fabricated by low pressure MOVPE. A 3 dB-bandwidth of 1.6 GHz and an open eye at 3.0 Gb/s NRZ modulation of the monolithically integrated photoreceiver were obtained by on-wafer characterization.

I. Introduction

Very fast InP-based opto-electronic devices operating at light wavelengths of 1.3 µm to 1.6 µm are needed for fibre-optic communications and future optical networks. Due to the reduction of parasitics the integration of these devices in OEICs (Opto-Electronic Integrated Circuits) is expected to improve the performance of gigabit per second systems as compared to hybrid circuits. In addition a reduction of cost is awaited which might be obtained even with a low complexity InP-OEIC in connection with an electronic Si-IC e.g. by flip-chip technique. So in the last few years increasing interest has been given to the study of receiver-OEICs.

Single InP-based devices are known to be well suited for very high frequency operation. A 3 dB-bandwidth of about 60 GHz for pin-diodes /1/ and about 100 GHz for MSM detectors /2/ have been reported, although the interpretation of these results for data transmission is under discussion /3/. Transistor short circuit current gain cut-off frequencies of 170 GHz at InGaAs-HBTs /4/ and 250 GHz at InAlAs-HEMTs /5/ have been demonstrated. But the technology for these devices is not applied for receiver-OEICs in most cases up to now and most of the OEICs do not use negative feedback to achieve the highest possible bandwidth. The best results for InP-based receiver-OEICs - built with various integration concepts - exhibit e.g. a 5 Gb/s-operation of InP/InGaAs-HBTs with a pin-photodiode /6/ and a

3 dB-bandwidth of 6 GHz of InAlAs/InGaAs-HEMTs with a pin-diode /7/.

II. Epitaxy and Device Preparation

We present results achieved with receiver-OEICs consisting of InGaAs pin-photodiodes and InAlAs/InGaAs HEMTs grown by low pressure metalorganic vapor phase epitaxy (MOVPE) on semi-insulating InP substrates. Growth conditions of the InAlAs/InGaAs-layers were optimized and an excellent mobility in the 2DEG of up to 11200 cm^2/Vs at 300 K (52000 cm^2/Vs at 77 K) was observed. Single pin-diodes and HEMTs were fabricated by standard processes which are described elsewhere /8/. Typical dark currents of pin-diodes with 45 µm diameter were below 10 nA, capacitances were in the order of 200 fF, quantum efficiency was 75 % at 1.3 µm wavelength. The transconductance of a nominal 1 µm gate length HEMT was around 400 mS/mm, transit frequencies of more than 25 GHz were observed.

Zn-diffused pin-Diode   Schottky Gate HEMT
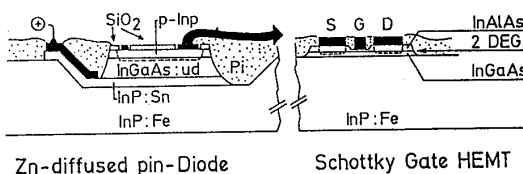
Fig. 1: Cross-section of a processed pin-HEMT wafer showing the pin-diode in the recess and the HEMT-layers outside.

To realize both devices on the same wafer the HEMT-layers were grown in a first epitaxial step. To align the surface of the pin-diodes and the HEMTs, recesses were etched by reactive ion etching before the growth of the pin-layers. Wet chemical etching

was used to remove the pin-layers on top of the HEMT-layers prior to the processing of the HEMTs /8/ (see Fig. 1). Then both devices were realized by standard processes.

III. On-wafer Characterization

The high frequency behaviour of the HEMTs was characterized by on-wafer S-parameter measurements in the frequency range of 50 MHz up to 26.5 GHz using a Cascade Wafer Probe Station and a HP 8510B Network Analyzer. Single HEMTs on the OEIC-wafer were used to measure the influence of the complete integration process on the performance of the transistors. We have found a decrease in the transit frequency for HEMTs on OEIC-wafers. In Fig. 2 the extrinsic transit frequency of the integrated HEMTs is shown as a function of gate-source voltage. Parameter is the drain-source voltage. Data were calculated from S-parameters measured by the bias sweep technique /9/. Values of up to 18 GHz were observed. This decrease of about 8 GHz compared to HEMTs on wafers without OEICs is mainly due to a difference in the gate length. The optical lithography on the non-ideal planar surface led to an enlargement of the gate length from 1 µm to about 1.6 µm, therefore the transit frequencies are in good agreement with the expected values. As can be seen in Fig. 2 moreover there is a broad range for the gate-source voltage for maximum transit frequency. This is important for a proper design of the circuit.
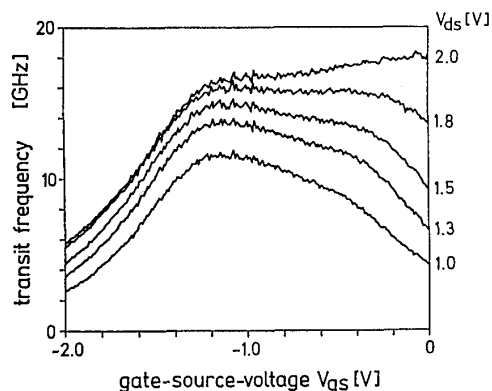
Fig. 2: Short circuit current gain cut-off frequency of an integrated HEMT as a function of gate-source voltage. Parameter is the drain-source voltage. Values were calculated from S-parameters measured by the bias sweep technique (/9/).

The detector slope responsivity - that means the ratio of electrical output current into the 50 Ω

measurement system to modulated optical input power - of the integrated pin-diode is depicted in Fig. 3 at reverse voltages of 1, 2 and 5 Volts. The measurement was performed on-wafer using the same equipment in addition with a HP 83420A Lightwave Test Set containing a 1300 nm wavelength Fabry-Perot laser as a calibrated modulated light
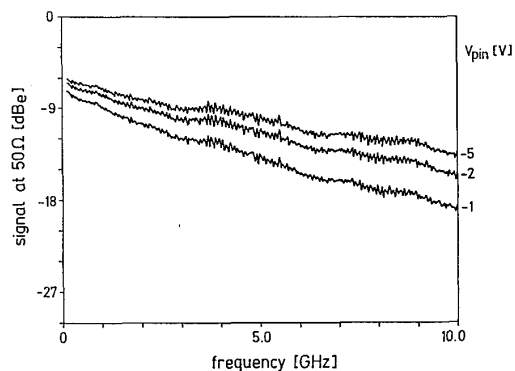
Fig. 3: O-E-transfer function of an integrated pin-diode. Parameter is reverse bias. Reference level is not calibrated.
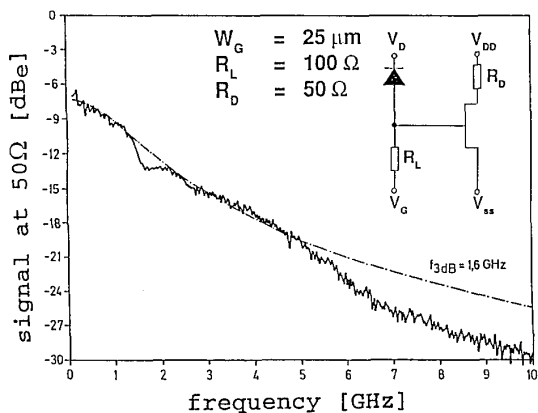
Fig. 4: O-E-transfer function of a pin-HEMT-OEIC. Parameter: V_D = - 5.0 V, V_{DD} = 1.30 V, V_G = 0.50 V. Reference level is not calibrated.

source. A 10 µm diameter lensed single-mode fiber was aligned above the wafer using a x-y-z-manipulator to illuminate the diode whereas a Cascade Probe Head was used to detect the electrical response. The 3 dB-bandwidth is in the order of 3 GHz which allows for operation in systems

up to 6 Gb/s.

The high frequency O-E-response of the complete receiver-OEIC was also measured on-wafer using the same equipment. Fig. 4 demonstrates the 3 dB-bandwidth of 1.6 GHz for the first, not yet optimized pin-HEMT-OEIC. The simple high impedance circuit can be seen as an inlet in Fig. 4. An improvement of the bandwidth is expected by the reduction of the capacitance and series resistance of the pin-diode.
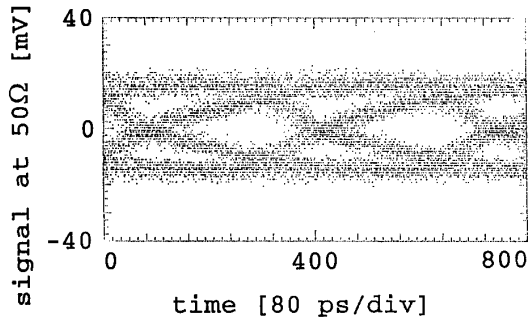
Fig. 5: Eye diagram of the monolithic photoreceiver measured on-wafer at 3.0 Gb/s pseudo-random NRZ modulation.

The bandwidth is in good agreement with a large-signal experiment performed on-wafer also. An Anritsu Pattern Generator MP 1701A was used to modulate a SEL 1.55 µm wavelength 10 Gb/s-laser-module with a pseudo-random NRZ bit pattern. The optical bit stream generated by the laser-modul was coupled by the lensed fiber to the pin-diode of the receiver-OEIC. The electrical response was analyzed by a HP 54120T Sampling Oscilloscope generating eye-diagrams in on-wafer experiments. As can be seen in Fig. 5 the eye is clearly open at 3.0 Gb/s which corresponds excellently with the measured bandwidth.

IV. Optimization and Discussion

The performance of the presented receiver-OEIC is partially limited by the bandwidth of the pin-diode. So a separate pin-diode run was performed to improve the pin-diode. A 3 dB-bandwidth of 10 GHz was achieved indicating a better contact and series resistance.

For an application in a next future low cost and low complexity receiver-OEIC in a first step the sensitivity might be more essential than extremly high speed. This sensitivity is limited by the receiver input leakage current at lower bit rates and by the input capacitance

of the receiver at higher bitrates. Separate HEMT runs were performed and doping density and doping layer thickness were varied to study the influence of the layer sequence on the device characteristics /10/. As can be seen in Fig. 6 as the first result the transit frequencies of 1 µm gate length HEMTs are improved to values of up to 33 GHz. Moreover from comparison of the maximum cut-off frequency obtained with samples with high doping ($5*10^{18}$cm^{-3},
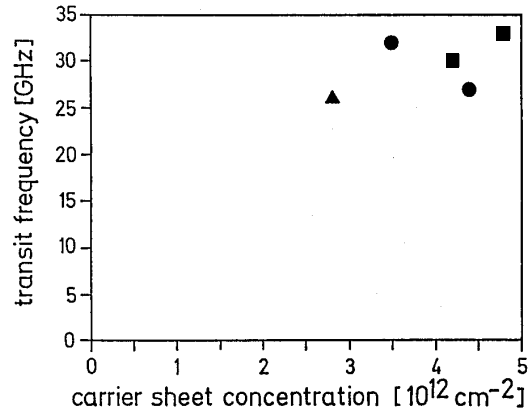
Fig. 6: Short circuit current gain cut-off frequency of separately processed HEMTs calculated from measured S-parameters vs. carrier sheet concentration. Dots ($2.8*10^{18}$cm^{-3}), triangles ($3.5*10^{18}$ cm^{-3}) and squares ($5*10^{18}$ cm^{-3}) refer to dopant concentration in the dopant layer.
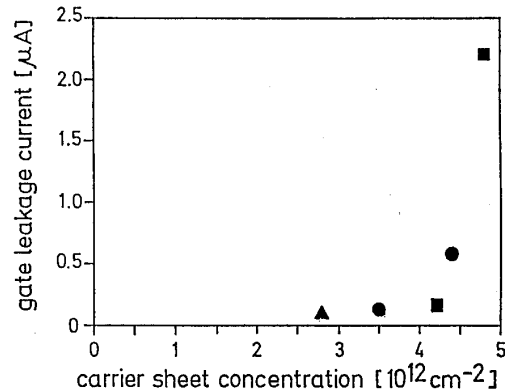
Fig. 7: Gate leakage current of separately processed HEMTs at optimum transit frequency bias point vs. carrier sheet concentration. Dots ($2.8*10^{18}$cm^{-3}), triangles ($3.5*10^{18}$ cm^{-3}) and squares ($5*10^{18}$ cm^{-3}) refer to dopant concentration in the dopant layer.

569

transit frequency 33 GHz) and with low doping $(2.8*10^{18}$ cm^{-3}, transit frequency 32 GHz) it is obvious that there is no need for extremely high doping for HEMTs with gate lengths of 1 μm.

As can be seen in Fig. 7 a medium doping concentration and a carrier sheet concentration of around $3*10^{12}$ cm^{-2} allows very low gate leakage currents in the order of 50 nA for a $1*100$ μm^2 gate at optimum transit frequency bias point. As an additional result a good compromise is achieved between high frequency performance and leakage current, so that a good sensitivity can be expected at low bit rates. More than that - as discussed in more detail in /10/ - the gate capacitance - which is in the order of 300 fF - shows also no significant dependence on the carrier sheet concentration; so a good sensitivity is expected for higher bitrates, too.

Acknowledgement

References

/1/   Tucker, R. S. et al., Electron. Lett., **EL-22**, 917, 1986.

/2/   B. J. van Zeghbroeck et al., IEEE Electron. Dev. Lett., **vol. 9**, pp. 527-529, 1988.

/3/   D. Kuhl et al., Conf. Proc of the 17th European Conference on Optical Communication ECOC '91, Paris, France, pp. 257-260, 1991.

/4/   Y.-K. Chen et al., IEEE Electron. Dev. Lett., **vol. 10**, pp. 267-269, 1989.

/5/   Mishra, U. et al., in *1989 IEDM Tech. Dig.*, Dec. 1989.

/6/   Chandrasekhar, S. et al., IEEE Photon. Technol. Lett., **vol. 3**, pp. 823-825, 1991.

/7/   Yano, H. et al., in *Technical Digest on Optical Fiber Communication*, 1991.

/8/   J.-H. Reemtsma et al., Conf. Proc. of the Third Int. Conf. InP & Related Materials, Cardiff, Wales, U.K. , pp. 114-117, 1991.

/9/   B. Hughes and P. Tasker, IEEE Trans. Electron. Devices, **vol. 36**, pp. 2267-2273, 1989.

/10/   J.-H. Reemtsma et al., accepted for publication in the Conf. Proc. of the Fourth Int. Conf. InP & Related Materials, Newport, Rhode Island, U.S.A., 1992.